IJASRaR
ISSN: 3062-2751

International Journal of Applied Sciences and Radiation Research

Vol. 3-No.1 (2026) pp. 59-63 https://doi.org/10.22399/ijasrar.69

Research Article *www.ijasrar.com*

Theoretical Assessment of Photon Shielding Parameters of a Nominal Glass Composition

Ahmed Boutejdar*

German Research Foundation Bonn-Braunschweig (DFG), Germany
* **Corresponding Author Email:** boutejdar69@gmail.com- **ORCID:** 0000-0002-7030-6350

Article History:

Received: Sep. 03, 2026
Revised: Oct. 25, 2026
Accepted: Oct. 29, 2026

Keywords:

Gamma-ray shielding;
glass composition;
mass attenuation coefficient

Abstract: This study presents a theoretical assessment of the photon attenuation and fast-neutron shielding parameters reported for a nominal $40MgO–22.5B_2O_3–30SiO_2–7.5La_2O_3$ (mol%) glass composition. The supplied spreadsheet contains 101 energy records spanning 0.005888–15 MeV and reports mass and linear attenuation coefficients, half- and tenth-value layers, mean free path, effective atomic number. The mass attenuation coefficient decreases from a maximum of 191.04 $cm^2\ g^{-1}$ at 0.005899 MeV to 0.02860 $cm^2\ g^{-1}$ at 10 MeV, while the half-value layer increases from 0.00116 cm to 7.7189 cm. The effective atomic number varies with photon energy, reaching 38.35 at 0.0395 MeV and a minimum of approximately 14.32 near 1.30 MeV. These trends indicate strong energy- and penetration-depth dependence.

1. Introduction

The development of materials that attenuate ionizing radiation is important in medical imaging, radiotherapy, nuclear technology, industrial radiography, and radiation-protection facilities. Glass-based shielding materials are of particular interest because their composition can be tailored and, in suitable systems, transparency can be combined with photon attenuation. The shielding response of a glass depends on its elemental composition, density, and the energy of the incident photon. Consequently, a single attenuation value is not sufficient to describe performance over a broad energy range [1,2].

The mass attenuation coefficient (MAC) is a fundamental descriptor of photon interaction probability per unit mass thickness. From MAC and material density, the linear attenuation coefficient (LAC) can be obtained; the half-value layer (HVL), tenth-value layer (TVL), and mean free path (MFP) then provide thickness-based descriptions of attenuation. Effective atomic number and effective electron density are also used to characterize the energy-dependent interaction response of multicomponent materials. Photon interaction databases such as NIST XCOM provide cross sections and attenuation coefficients for elements, compounds, and mixtures over a wide energy range [3].

Computational tools have made it possible to evaluate several shielding and dosimetry parameters consistently, including MAC, LAC, HVL, TVL, MFP, effective atomic number, and buildup factors. The Phy-X/PSD platform, for example, was developed to calculate a broad set of photon shielding parameters and fast-neutron removal cross sections [1]. Previous theoretical studies have applied these approaches to borate and silicate glass systems and have emphasized the importance of composition and photon energy when comparing shielding performance [4,5].

The present work analyzes the numerical dataset supplied in the Excel worksheet for the nominal $40MgO–22.5B_2O_3–30SiO_2–7.5La_2O_3$ composition. The objective is to describe the energy dependence of photon attenuation, thickness-related shielding parameters, effective atomic number, buildup factors, and fast-neutron removal cross section. The work is limited to analysis of the supplied calculated outputs; the spreadsheet does not document sample preparation, experimental measurements, or the specific calculation software.

2. Materials and Methods

The copyright of the published article belongs to its author under CC BY 4.0 license. To view a copy of this licence, visit http://creativecommons.org/licenses/by/4.0/

The worksheet header identifies the nominal composition as $40MgO + 22.5B_2O_3 + 30SiO_2 + 0Al_2O_3 + 7.5La_2O_3 + 0Y_2O_3$, with the fractions expressed on a molar basis. The reported density is 3.14 g cm^{-3}. The energy-dependent dataset contains 101 records between 0.005888 and 15 MeV.

A data-integrity check was performed by comparing the nominal molar composition in the worksheet header with the compound weight fractions listed in the composition table. Weight fractions expected from the nominal molar formula were calculated from the molar fractions and formula masses. This check is essential because mixture-based attenuation calculations depend on the elemental or compound fractions supplied to the calculation procedure [3].

For a narrow-beam photon attenuation model, the transmitted intensity I through a material thickness x is related to the incident intensity I_0 by the exponential attenuation relation:

$$I = I_0 \exp(-\mu x) \quad (1)$$

where μ is the linear attenuation coefficient. The relationship between MAC (μ/ρ), LAC, and density ρ is $\mu = \rho(\mu/\rho)$. The thickness parameters are calculated from the attenuation coefficient as:

$$HVL = \ln(2)/\mu; \quad TVL = \ln(10)/\mu; \quad MFP = 1/\mu. \quad (2)$$

3. Results and Discussions

The comparison in Table 1 confirms that the worksheet composition requires verification before publication. The present article therefore avoids attributing the reported attenuation values to a confirmed, experimentally prepared glass formulation.

Table 1. *Comparison of nominal and reported compound fractions.*

Compound	Nominal mol%	Worksheet wt%	Wt% from nominal formula
MgO	40.0	4.01	21.71
B2O3	22.5	3.90	21.10
SiO2	30.0	4.48	24.28
Al2O3	0.0	25.36	0.00
La2O3	7.5	6.08	32.91
Y2O3	0.0	56.17	0.00

The MAC exhibits a pronounced energy dependence. Its maximum value in the dataset is 191.04 $cm^2\ g^{-1}$ at 0.005899 MeV, whereas its minimum is 0.02860 $cm^2\ g^{-1}$ at 10.000 MeV. At 15 MeV, the MAC is 0.02916 $cm^2\ g^{-1}$. The sharp reduction from the low-energy region to the MeV region indicates that the material's photon attenuation is strongly dependent on incident energy. This general behavior is consistent with the energy dependence of photon interaction cross sections described in XCOM-based evaluations [3].

The LAC follows the same overall trend because it is related to MAC through the reported density. The LAC reaches approximately 599.88 cm^{-1} at 0.005899 MeV and decreases to approximately 0.08980 cm^{-1} at 10 MeV. Figure 1 shows the energy dependence of MAC on logarithmic axes. The low-energy attenuation values should be interpreted with care because composition and absorption-edge effects can strongly influence attenuation coefficients in this region [3]. The HVL increases from a minimum of 0.001155 cm at 0.005899 MeV to a maximum of 7.7189 cm at 10.0 MeV. The maximum TVL and MFP also occur at 10 MeV, reaching 25.642 cm and 11.136 cm, respectively. At 15 MeV, the reported HVL, TVL, and MFP are 7.570 cm, 25.148 cm, and 10.921 cm. These results indicate that substantially greater thickness is required to attenuate higher-energy photons.

Table 2. *Selected photon shielding parameters at representative energies.*

Energy (MeV)	MAC (cm^2/g)	HVL (cm)	MFP (cm)	Zeff
0.005899	191	0.001155	0.001667	28.661
0.015	15.59	0.01416	0.02043	30.968
0.05	3.435	0.06427	0.09271	37.163
0.511	0.086	2.567	3.703	14.795
0.6617	0.07494	2.946	4.25	14.557
1.173	0.05567	3.965	5.72	14.325
1.333	0.05211	4.236	6.112	14.317
15	0.02916	7.57	10.92	18.854

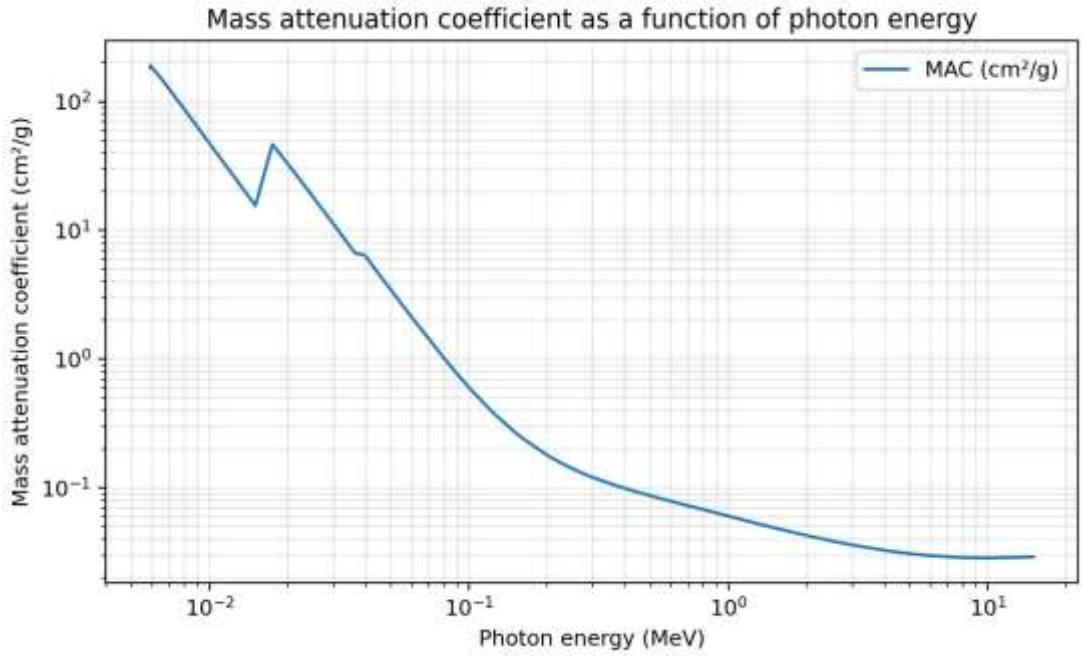

Figure 1. *Mass attenuation coefficient as a function of photon energy.*

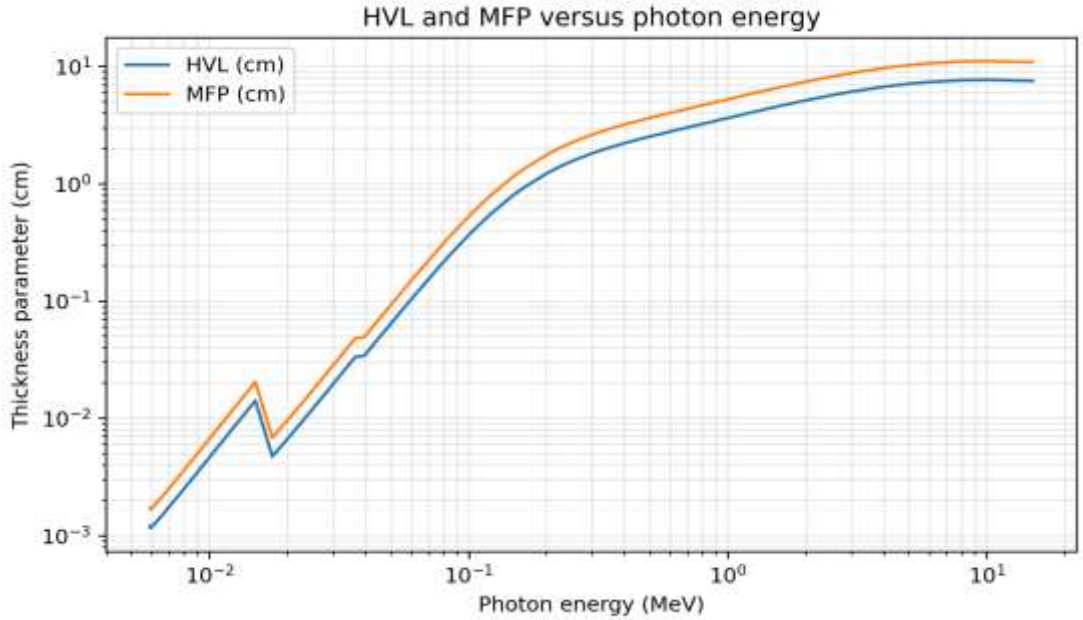

Figure 2. *Half-value layer and mean free path as functions of photon energy.*

The effective atomic number varies non-monotonically with photon energy. It reaches a maximum of 38.35 at 0.0395 MeV and a minimum of 14.32 at 1.299 MeV. This behavior reflects the changing relative contribution of photon interaction processes as energy changes. The effective atomic number is therefore not a fixed material constant and should be reported together with the photon energy. Similar energy-dependent Zeff analyses are commonly used in comparative studies of glass shielding systems and also other materials and parameters[4-20].

4. Conclusions

The MAC decreases substantially with increasing photon energy, while HVL and MFP generally increase, indicating that higher-energy photons require greater shielding thickness. The effective atomic number varies with energy.

A major limitation is the inconsistency between the nominal molar formula and the compound weight fractions in the worksheet.

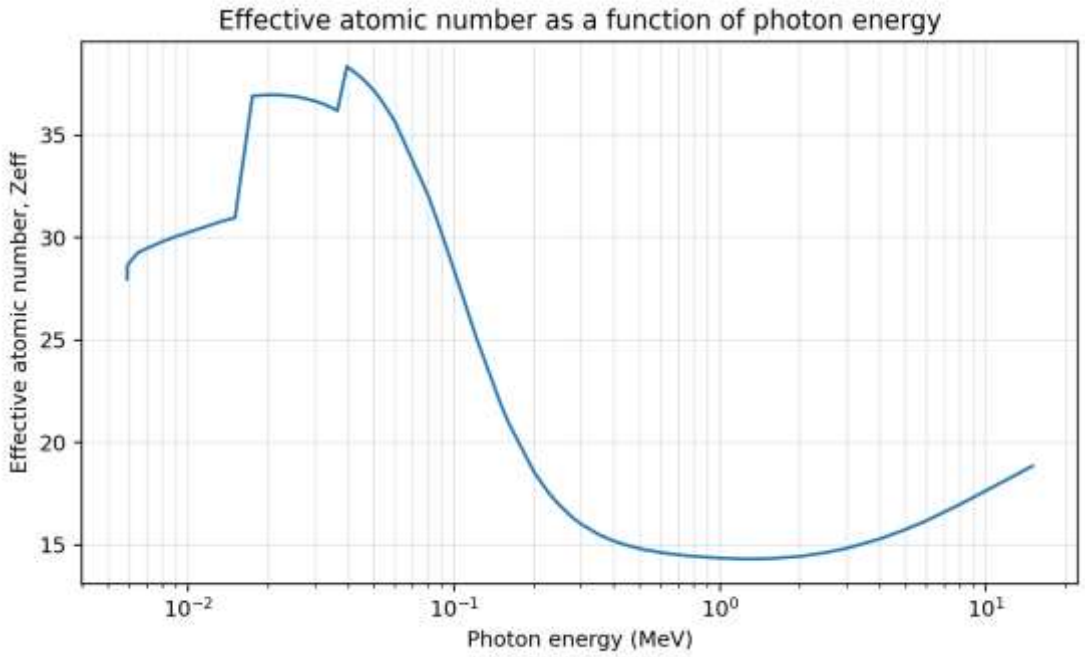

***Figure 3**. Effective atomic number as a function of photon energy.*

Author Statements:

- **Ethical approval:** The conducted research is not related to either human or animal use.
- **Conflict of interest:** The authors declare that they have no known competing financial interests or personal relationships that could have appeared to influence the work reported in this paper
- **Acknowledgement:** The authors declare that they have nobody or no-company to acknowledge.
- **Author contributions:** The authors declare that they have equal right on this paper.
- **Funding information:** The authors declare that there is no funding to be acknowledged.
- **Data availability statement:** The data that support the findings of this study are available on request from the corresponding author. The data are not publicly available due to privacy or ethical restrictions.
- **Use of AI Tools:** The author(s) declare that no generative AI or AI-assisted technologies were used in the writing process of this manuscript

References

[1] Şakar, E., Özpolat, Ö. F., Alım, B., Sayyed, M. I., & Kurudirek, M. (2020). Phy-X/PSD: Development of a user friendly online software for calculation of parameters relevant to radiation shielding and dosimetry. Radiation Physics and Chemistry, 166, 108496. https://doi.org/10.1016/j.radphyschem.2019.108496

[2] Berger, M. J., Hubbell, J. H., Seltzer, S. M., Chang, J., Coursey, J. S., Sukumar, R., Zucker, D. S., & Olsen, K. (2010). XCOM: Photon Cross Sections Database (NIST Standard Reference Database 8, Version 1.5). National Institute of Standards and Technology. https://doi.org/10.18434/T48G6X

[3] Berger, M. J., & Hubbell, J. H. (1987). XCOM: Photon cross sections on a personal computer (NBSIR 87-3597). National Bureau of Standards. https://doi.org/10.6028/NBS.IR.87-3597

[4] Bagheri, R., & Shirmardi, S. P. (2021). Gamma-ray shielding studies on borate glasses containing BaO, Bi_2O_3, and PbO in different concentrations. Radiation Physics and Chemistry, 184, 109434. https://doi.org/10.1016/j.radphyschem.2021.109434

[5] Ruengsri, S. (2014). Radiation shielding properties comparison of Pb-based silicate, borate, and phosphate glass matrices. Science and Technology of Nuclear Installations, 2014, Article 218041. https://doi.org/10.1155/2014/218041

[6] Seher Polat, Mucize Sarıhan, Roya Boudaghi Malidarreh3, Sabiha Anas Boussaa, Nurdan Karpuz, & Nuray Kutu. (2026). ANN Prediction of Linear Attenuation Coefficients for 40MgO–30B2O3–30SiO2 System. *International Journal of Applied Sciences and Radiation Research* , *3*(1). https://doi.org/10.22399/ijasrar.56

[7] Lotfihagh, A., & Roya Boudaghi Malidarreh. (2025). FLASH Radiotherapy: Biochemical Mechanisms, Current Evidence, and Remaining Challenges. *International Journal of Biological-Medical Science and Technology*, *3*(1). https://doi.org/10.22399/ijbimes.20

[8] Nasser Khidhr Alhazmi, Sultan Dagham Alanazi, Hammad Shabeeb A Alrowily, Khaled Fayez Alkhamsan, Fawaz Awad Dahisan Al-Rashidi, Al-Salem Sultan Mohammed, … Ahmed Ayyaf k AlQusayri. (2026). Radiation Safety Compliance and Protective Practices Among Radiologic Technologists. *International Journal of Computational and Experimental Science and Engineering*, *10*(4). https://doi.org/10.22399/ijcesen.4664

[9] Demet Sarıyer. (2025). A FLUKA-Based Study on the Effect of Boron-Enhanced Concrete on Secondary Neutron Dose under Proton Beam Loss Scenarios. *International Journal of Natural-Applied Sciences and Engineering*, *3*(1). https://doi.org/10.22399/ijnasen.30

[10] Betul Cetin, Arzu Poyraz, & Melek Gul. (2026). Examination of the radiation absorption parameters of CuO coatings prepared at different ratios. *International Journal of Sustainable Science and Technology*, *4*(1). https://doi.org/10.22399/ijsusat.35

[11] Emikönel, S., & Akkurt, İskender. (2025). Radiation Shielding Properties of B2O3-Bi2O3 Glass . *International Journal of Computational and Experimental Science and Engineering*, *11*(2). https://doi.org/10.22399/ijcesen.2157

[12] SOYAL, H., & SARIHAN, M. (2025). Radiation Safety Awareness for Future Healthcare Workers: Educational and Legal Perspectives. *International Journal of Biological-Medical Science and Technology*, *3*(1). https://doi.org/10.22399/ijbimes.1

[13] Günoğlu, K., & Akkurt, İskender. (2024). Gamma-ray attenuation properties carbide compounds (WC, Mo2C, TiC, SiC, B4C) using Phy-X/PSD software. *International Journal of Applied Sciences and Radiation Research* , *1*(1), 1–8. https://doi.org/10.22399/ijasrar.6

[14] Demet Sarıyer, & Mustafa Emre Erbil. (2026). Comparative Analysis of Secondary Particle Production and Spatial Dose Distributions in Multilayer Concrete-Iron Shielding Systems for a 50 MeV Proton Accelerator Using FLUKA. *International Journal of Computational and Experimental Science and Engineering*, *12*(1). https://doi.org/10.22399/ijcesen.5083

[15] Sibel ÖZAVCI, & Betül ÇETİN. (2017). Experimental Investigation of Radiation Shielding Effect in Different Doped Slag Concrete. *International Journal of Sustainable Science and Technology*, *2*(1). https://doi.org/10.22399/ijsusat.23

[16] Nuray Kutu. (2026). Radiation Shielding Properties of recycled waste glass color doped powder cement pastes. *International Journal of Applied Sciences and Radiation Research* , *3*(1). https://doi.org/10.22399/ijasrar.55

[17] Sağlam, F., & Cetin, B. (2025). Investigation of Gamma Shielding Properties of Some Industrial Materials. *International Journal of Computational and Experimental Science and Engineering*, *11*(2). https://doi.org/10.22399/ijcesen.1357

[18] Menşure Canpolat, & Halil Soyal. (2025). The Relationship Between Radiation Safety and Ergonomics in Healthcare Workers: Comprehensive Protection Approaches. *International Journal of Biological-Medical Science and Technology*, *3*(1). https://doi.org/10.22399/ijbimes.21

[19] Betul Cetin, & Betul Sezer. (2025). Comparison of the radiation shielding effect of travertine and gasconcrete. *International Journal of Natural-Applied Sciences and Engineering*, *3*(1). https://doi.org/10.22399/ijnasen.31

[20] Waheed, F., Mohamed Abdulhusein Mohsin Al-Sudani, & Iskender Akkurt. (2025). The Experimental Enhancing of the Radiation Shield Properties of Some Produced Compounds. *International Journal of Applied Sciences and Radiation Research* , *2*(1). https://doi.org/10.22399/ijasrar.1